

Study the X-ray attenuation for a voltage range (20-35)Kv for copper-based smart alloys by adding silver and micro-particles

Mahmood Abraham Mahmed¹, Fareed Majeed Mohammed², Raed Najeeb Razoqi³

^{1,2}College of Science, Department of Physics, Tikrit University, Republic of Iraq.

³College of Engineering, Department of Mechanics, Tikrit University, Republic of Iraq.

Email: alkese015@gmail.com

DOI: 10.47750/pnr.2022.13.S06.466

Abstract

In this paper, the attenuation coefficients of X-rays for a range of voltages (20-35) kV were studied for copper-based alloys (Cu + 0.05 AL + 0.03 Ti) according to the order (A1,A2,A3,A4,A5), by adding percentages of silver (X=1,2,3,4,5)% with two particle sizes (Nano) and (Micro) to the alloy (Cu92-x +5%A1 +3%Ti+ Ag x) according to the orders (B1,B2,B3,B4,B5) and (C1,C2,C3,C4,C5) All alloys were sintered at (9000C) for a period of (4) hours.

The results showed a direct relationship between the attenuation coefficient and the compression pressure. At the operating voltage (20Kv), the linear attenuation was increased (53.6%) and the mass attenuation was (53.8%), the hardness increased by (45%) and the porosity decreased by (18%) when comparing the results of Alloy (A1). with (A5), respectively, and it was also found that the relationship is direct between the attenuation coefficient and the percentages of silver addition, as it was noticed that the linear and mass attenuation coefficients increased by (34.5%) (34%) when comparing the results of (B1) with (B5), respectively, and the increase is By (33.9%) (33.5%) when comparing the results of (C1) alloys with (C5), the hardness has increased by (33.4%) (32.2%) when comparing the average values of alloy results from (B1) to (B5) and alloys from (C1) to (C5) and the porosity decreased by (37.6%) (31%), respectively. The attenuation coefficient is inversely proportional to the operating voltage, as it decreased by (20%) when comparing the results of voltages (20Kv) with (35Kv) for alloy (B5) and decreased by (26.4%) for alloy (C5).

Keywords: smart alloys, linear and mass attenuation coefficient, hardness, porosity, operating voltage.

INTRODUCTION

Photon interactions with materials, absorption and penetration are important concepts, as photon interactions with materials are used in a wide range of sectors. The linear and mass attenuation coefficients and the mean free path have become a necessity for radiation protection, nuclear diagnostics, and radioactive dosimetry through the manufacture of protective shields from smart alloys [1,2].

Attenuation

When photons (X-rays) fall on the material, the photons are attenuated and this attenuation reduces the intensity of the photons as a result of interactions with the material. Composite materials and smart materials provide additional benefits in physical strength, transportability and chemical resistance, as there are three main processes for the interaction of (X-rays) with the material are the photoelectric phenomenon, Compton scattering and pair production, and pair production processes occur only for high energy (X-rays >1.022 Mev) as The sum of the processes (photoelectric phenomenon, Compton scattering and pair production) on photons (X-rays) leads to the removal of photons from the incident ray beam and is called linear attenuation coefficient (μ_L) and is given by the following relationship [3,4]:-

$$\mu_L = \sigma(\text{photoelectric}) + \sigma(\text{Compton}) + \sigma(\text{pair}) \dots\dots\dots (1)$$

σ = reaction cross-sectional area .

The thickness of the material (X) is measured in units (cm, mm) and the linear attenuation coefficient is measured in units (cm⁻¹, mm⁻¹) The linear attenuation coefficient depends on the energy of the incident photon and the atomic number (Z) of the medium. [5] :-

$$\mu_L = (\ln(I_0/I))/X \dots\dots\dots(2)$$

To obtain the mass attenuation coefficient (μ_m) in units (cm².gm⁻¹), the equivalent thickness is measured and given by the following relationship [5] :-

$$\mu_m = (\ln(I_0/I))/\rho X \dots\dots\dots(3)$$

Many researchers have resorted to studying X-ray attenuation using copper-based alloys, which is the focus of our current research. Researcher Apaydm Cengiz.G (and others) presented in 2009 a study on the mass attenuation coefficients, effective atomic number and electron density for copper-based alloys (Cu-Co-Ag), the results showed that the alloy is well absorbent in the energy range (1150 - 150) Kev [6] In 2011, the researcher (Fred et al.) presented an experimental study to measure the X-ray attenuation coefficients of some aluminum-based alloys. It was found that there is an inverse relationship between the grain size and the attenuation coefficients [7]. In 2012, (Farid et al.) investigated the oxidation effect of aluminum and some alloys on the attenuation coefficients within the range (35-20) kv A direct relationship was found between the attenuation coefficients and the oxidation time of aluminum and alloys [8]. In 2014, the researcher (Fried and others) presented a practical study to measure the attenuation coefficients for X-rays of the elements (Cu, Ti, Zn, Al) at different thicknesses. Awasarmo, Vishal.V and others) studied the attenuation coefficients, half thickness and free path rate of some shape memory alloys for the energy range (122-1330) Kev, as the study showed the dependence of the variation of the obtained values for all parameters on the photon energy [10]. In (2018) researcher Dapke Gopinath (P. et al) carried out several studies on the cross-section parameters of the attenuation of some shape-memory alloys in the energy range Kev-356-1330, and it was found that there is a good agreement between the experimental and theoretical values of the mass-attenuation coefficient of memory alloys (SMA), which are (AlNi), (FeTi), (CuZn), (CuSn) and (FeCrNiMO), as well as experimentally obtaining some relevant parameters using the values obtained from the attenuation coefficients at The Photon (1330 - 356 Kev) [11]. In 2018, the researcher (Fried and others) presented a study to measure the attenuation coefficients of X-rays for the element (Cu, Zn) and zinc alloys of different thicknesses. It was found that the proportion is directly between the thickness and the logarithm of the absorbance at an operating voltage (20Kv) for an alloy of brass (Cu +30%Zn) [12] In 2021, the researcher (Fred and others) studied the effect of shape memory alloys used as shields from radiation effects in terms of attenuation coefficients. Thickness (0.4 cm) The hardness increased and the porosity decreased in addition to the increase of the linear and mass attenuation coefficients when exposed to atomic and nuclear radiations [13].

shape memory alloys

Shape memory alloys (SMAs) represent a unique class of materials that possess properties such as shape memory effect, superior flexibility and high resistance to corrosion and fatigue. Some copper alloys are designed for use in safety and protection devices to stop the flow of toxic or flammable gases and have also been used in structural or The semi-structure to improve its resistance in addition to its use in the connections designated for air conditioning systems for its ability to remember the shape when heated to high temperatures and return to its original shape after cooling. The basis of this effect is the transformation of alloys from the martensite phase to the austenite phase [14,15].

Experimental part

1- Preparation of samples

Powder metallurgy technology was used to prepare the alloys under study (the alloy components have different melting points and different densities, as this technology was able to produce complex parts that require high accuracy in addition to effectively controlling the properties [16] by weighing the alloy components according to volumetric ratios. By means of an electronic balance, the alloys were encoded as shown in Table (1). The components of each sample were individually ground and mixed at an angular velocity of (500 rad/sec) for (0.5 h) according to [17], the components of the samples were pressed into a steel mold on Cold in one direction at a different pressure of (200-600) Mpa and keeping for a period of (2 min) for each sample and with a constant thickness of (0.6 cm) using a device type (HERZOG TP 20 P) [17]. Variable proportions (1-5)% of

silver with a particle size (Nano) were individually added to the (A5) alloy at a constant pressing pressure (600 Mpa) for a period of (2 min) and for a constant thickness (0.6Cm), the alloys (B1,B2,B3,B4,B5) were prepared The same process was repeated by adding the same proportions of silver with a particle size (micro) to the alloy (A5), thus the alloys (C1, C2, C3, C4, C5) were prepared, and cylindrical samples with a diameter of (1.2) were obtained. Cm), the samples were sintered at (900 0C) for (4 hour) then slow cooling to a temperature of (25 0C), taking into consideration their protection from oxidation according to [18,19].

Table (1): Samples symbol, volume ratio, thickness and pressing pressure.

Code	Cu (%)	Al (%)	Ti (%)	Ag % Micro	Ag % Nano	P(Mpa)	T (Cm)	
A	A 1	92	5	3	-	-	200	0.6
	A 2	92	5	3	-	-	300	0.6
	A 3	92	5	3	-	-	400	0.6
	A 4	92	5	3	-	-	500	0.6
	A 5	92	5	3	-	-	600	0.6
B	B 1	91	5	3	-	1	600	0.6
	B 2	90	5	3	-	2	600	0.6
	B 3	89	5	3	-	3	600	0.6
	B 4	88	5	3	-	4	600	0.6
	B 5	87	5	3	-	5	600	0.6
C	C 1	91	5	3	1	-	600	0.6
	C 2	90	5	3	2	-	600	0.6
	C 3	89	5	3	3	-	600	0.6
	C 4	88	5	3	4	-	600	0.6
	C 5	87	5	3	5	-	600	0.6

2- Analysis (EDX) and Microscopy (FeSEM)

The samples were prepared to be ready for the (EDX) and (Fe sem) examination. Figures (1-5) show the results of the examination.

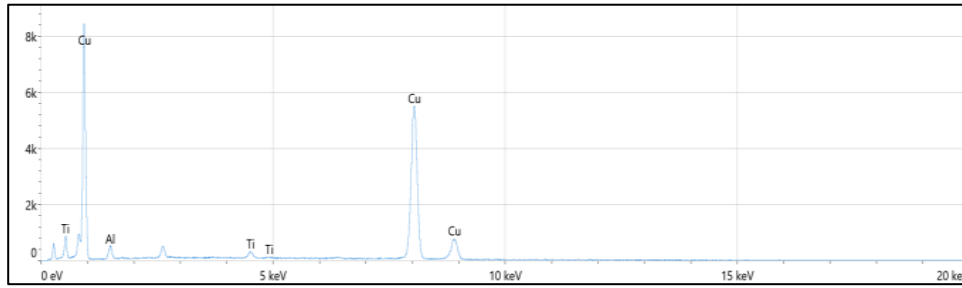


Figure (1) The distribution of the elements for checking (EDX) for alloy (A5) at compressive pressure (600Mpa) and thickness (0.6 cm).

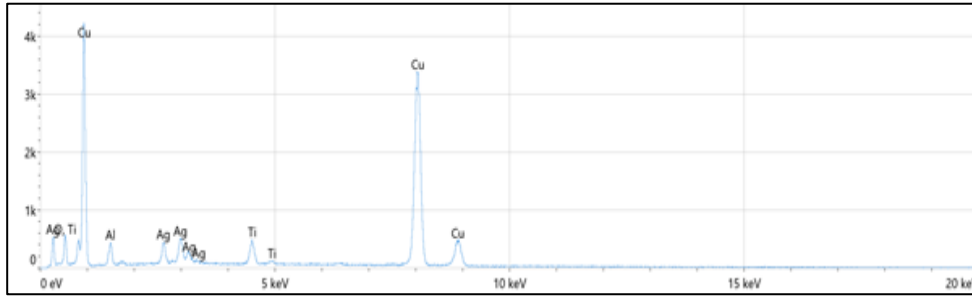


Figure (2) The distribution of the elements for the EDX examination of the base alloy (B5) at a compressive pressure of (600mpa) and a thickness of (0.6 cm)

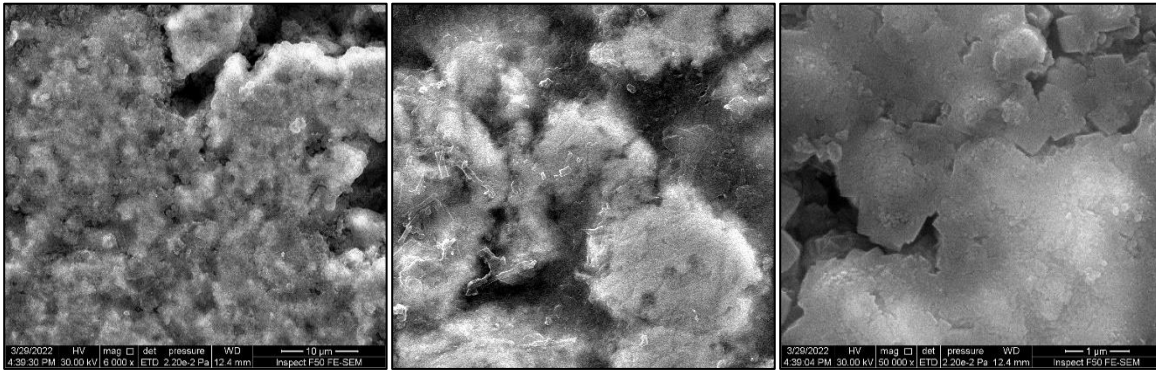


Figure (3) Scanning electron microscope (FeSem) images of the base alloy (A5) at a compressive pressure (600Mpa)

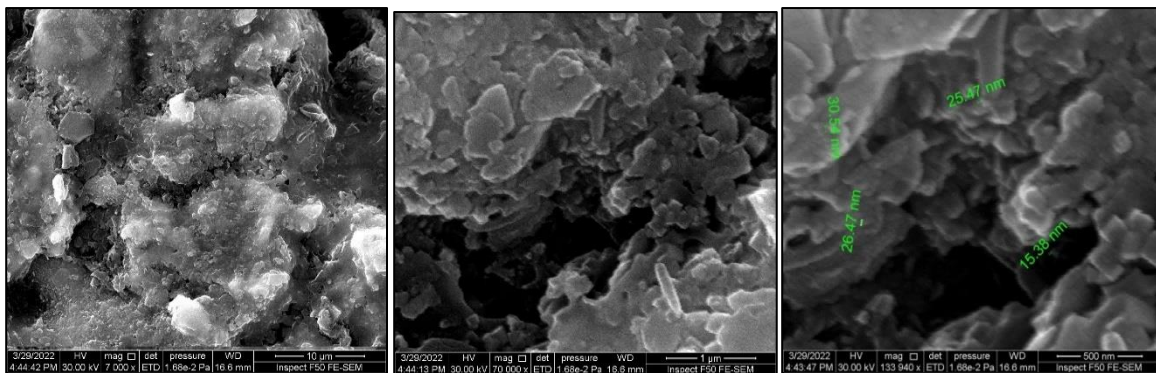


Figure (4) Scanning electron microscope (FeSem) images of the base alloy (B5) at a compressive pressure (600Mpa).

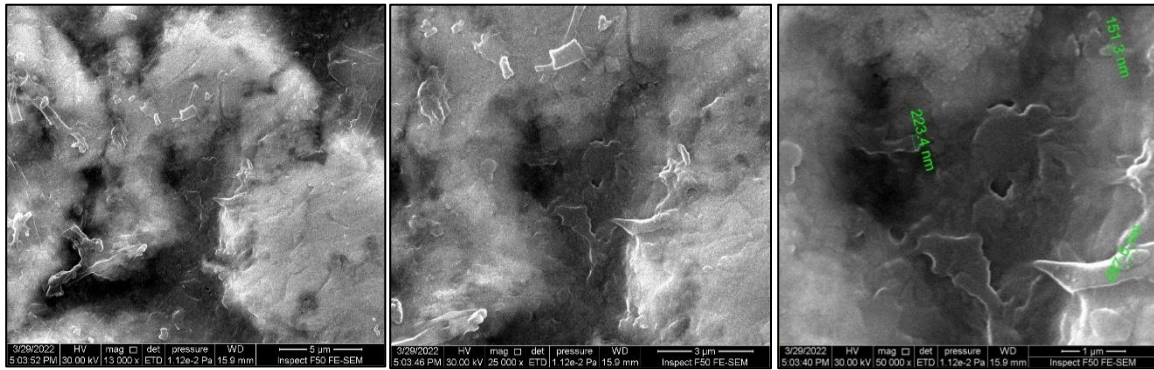


Figure (5) Scanning electron microscope (FeSem) images of the base alloy (C5) at a compressive pressure (600Mpa).

3- Experimental density and true porosity

The practical density and real porosity were calculated according to Archimedes' theory (ASTM B962-8), as equations (1) (2) (3) were used to find the experimental and theoretical density and porosity of alloys [20]:

$$E.D = \frac{M_a}{(M_i - M_a)} \rho_w \dots\dots\dots(1)$$

$$T.D = \sum \rho_i \cdot X_i \dots\dots\dots(2)$$

$$p = [1 - (E.D)/(T.D)] \cdot 100\% \dots\dots\dots(3)$$

As (M_a) the weight of the sample after drying it inside the electric furnace, (M_i) the weight of the sample while it is suspended and immersed in distilled water (ρ_w) the density of water, (X_i) the ratio of each element in the alloy, (ρ_i) the density of each element.

4- Hardness test

A Vickers hardness meter (Hv) was used to measure the hardness of the samples. The surface of the sample was prepared using a graded smoothing paper of silicon carbide, with measurements (800, 1000, 1500, 2000, 2500), and a load of (500 gm) was applied through the suture tool for a period of (5 sec) and the suture tool was lifted and the resulting effect diameter was measured on the surface of the sample, and the process was repeated five times for different areas that included the surface area.

5 - X-ray diffraction (XRD)

An X-ray diffraction machine (SHEMADZU) XDR-6000 was used [9].

6- Attenuation measurements of radiation

6-1 X-ray

X-ray attenuation measurements were made for samples of the alloys under investigation using the LEYBOLD PHYWE X-ray machine [21].

Results and discussion

1- X-ray diffraction (XRD)

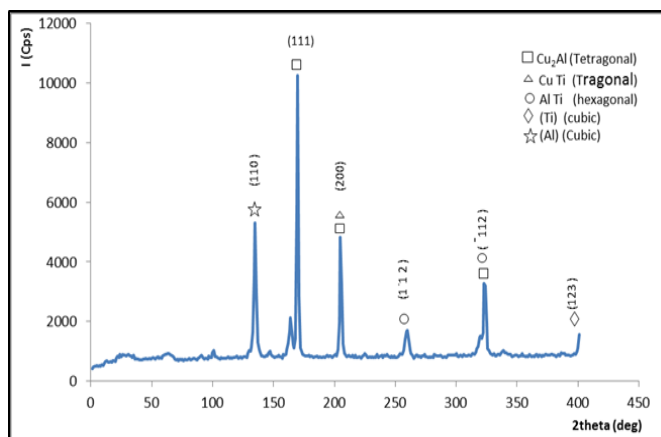


Figure (6) X-ray diffraction of (A5) alloy.

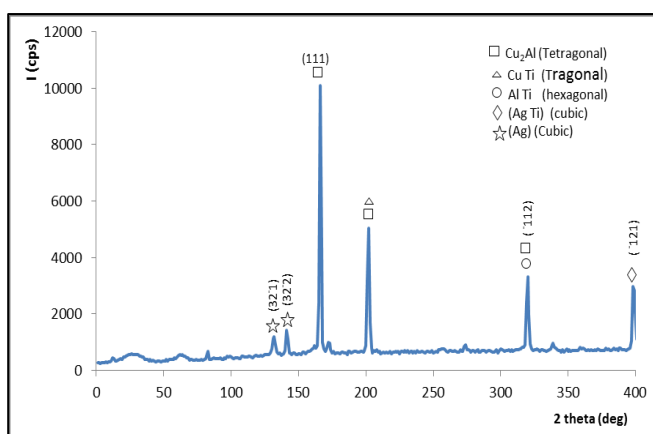


Figure (7) X-ray diffraction of (B5) alloy .

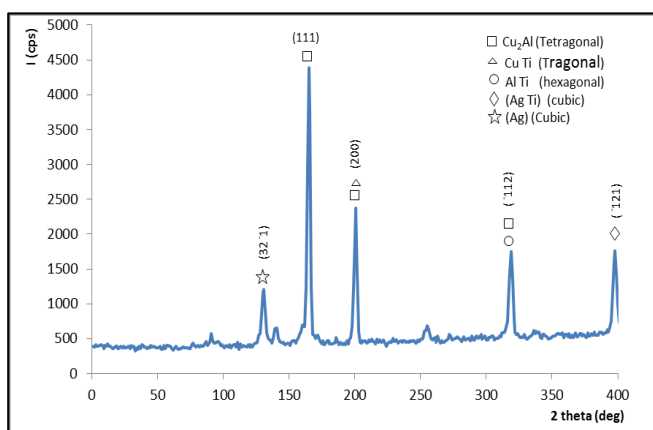


Figure (8) X-ray diffraction of (C5) alloy .

Figures (6-8) shows the results of the X-ray diffraction examination for alloys (A5), (B5) and (C5). It was found from the figures that The crystal growth of the phases and their different formations formed through data analysis had a significant impact on increasing the hardness and decreasing the percentage of porosity , This is attributed to the addition of silver and the size of its particles.

2- Linear and mass attenuation coefficients for X-rays .

2-1 Attenuation coefficients for alloys (A1,A2,A3,A4,A5).

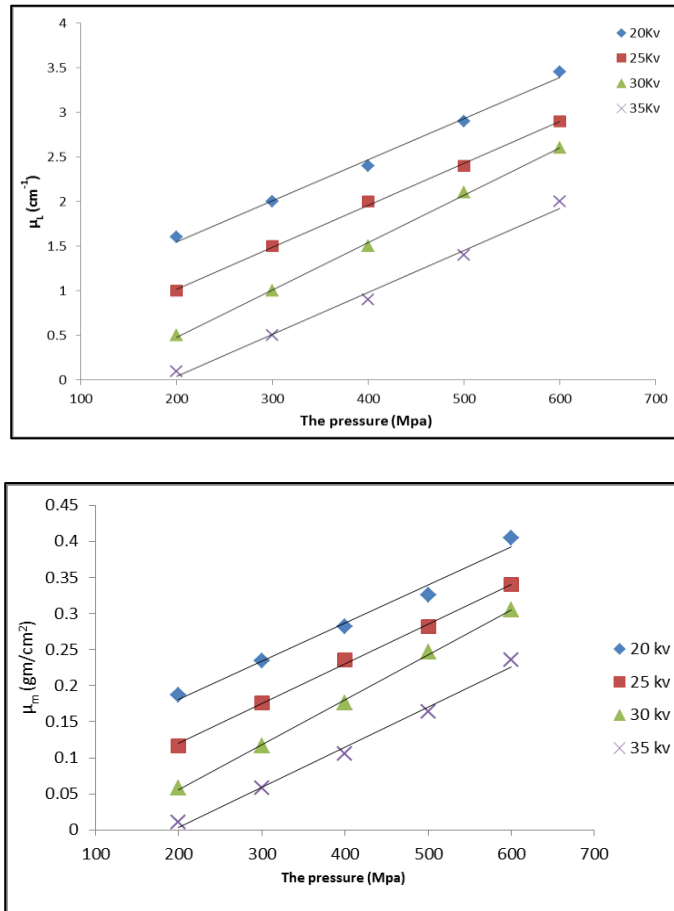


Figure (9) The relationship between the linear attenuation coefficient (μ_L) and compressive stress for alloys (A1,A2, A3, A4, A5) At a thickness of (0.6 cm) for a voltage range of (20,25,30,35)Kv .

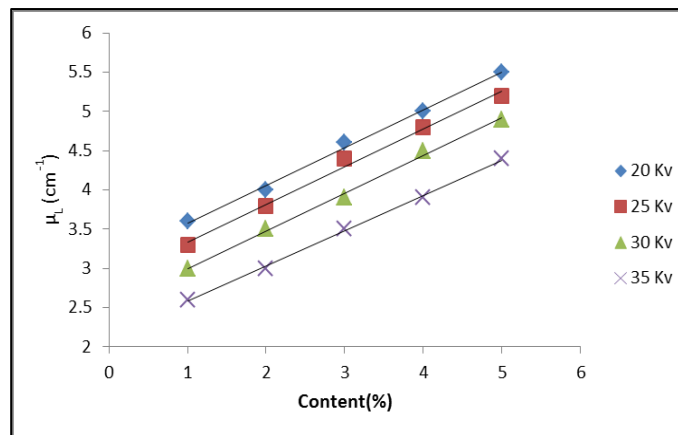


Figure (10) The relationship between the mass attenuation coefficient (μ_m) and compressive stress for alloys (A1,A2,A3,A4, A5) At a thickness of (0.6 cm) for a voltage range of (20,25,30,35)Kv .

Figures (9) and (10) show the relationship between the coefficients of linear and mass attenuation and compression pressure (200,300,400,500,600)Mpa for the base alloy (Cu-Al-Ti) and the range of operating voltages (20, 25, 30, 35) Kv as it was found that the relationship is direct between the coefficients of Attenuation Coefficient and Compressive Pressure The best compressive pressure for the base alloy is (600Mpa), which represents alloy (A5), as this alloy is considered as the best alloy for X-ray attenuation. The linear and mass attenuation coefficients increase by (53.6%) (53.8%) when comparing the attenuation results for alloy (A5) with (A1), respectively, and for operating voltage ((20Kv). The reason for the increase in the linear and mass attenuation coefficients is due to the increase in bulk density, hardness and compressive pressure, which leads to a reduction in the distances between atoms and a decrease in the porosity . It was found that there is an inverse relationship between the attenuation coefficients and the operating voltage, as the linear attenuation coefficient of the alloy (A5) decreased by (40%) when the operating voltage was increased from (20Kv) to (35Kv).

2-2 Linear and mass attenuation coefficients (μ_L , μ_m) for alloys (B1,B2,B3,B4,B5).

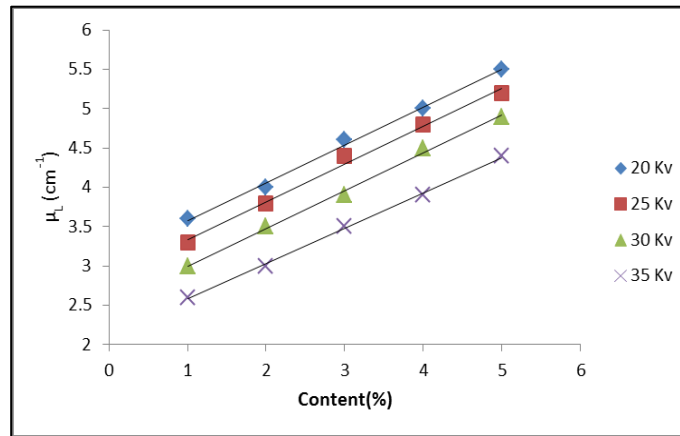


Figure 11: The relationship between the linear attenuation coefficient (μ_L) and the percentages of silver in the particle Nano size of (B1,B2,B3,B4,B5) alloys at a thickness of (0.6 Cm) for the voltage range (20,25,30, 35) kv.

Figure (11) shows the behavior of the relationship between the linear attenuation coefficient and the silver content (Nano particle) for (B1, B2, B3, B4, B5) alloys. It was found that the linear attenuation coefficient increases by (34.5%) when the silver content of the (B1) alloy is increased. to (B5), since silver leads to filling the voids in the alloy and increasing compaction, which leads to an increase in practical density and hardness, in addition to a decrease in porosity.

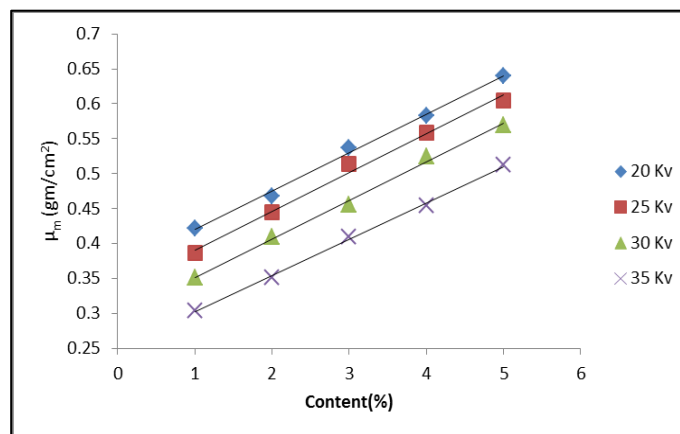


Figure 12: The relationship between the mass attenuation coefficient (μ_m) and the percentages of silver of (B1,B2,B3,B4,B5) alloys at a thickness of (0.6 Cm) for the voltage range (20,25,30, 35) kv.

Figure (12) shows the direct relationship between the mass attenuation coefficient and the silver content of the alloys (B1, B2, B3, B4, B5), as the mass attenuation coefficient increases by (34%) when the silver content is increased from (1-5)% to the effect of silver particles Its role is to fill in the blanks.

2-3 Linear and mass attenuation coefficients (μ_L , μ_m) for alloys (C1,C2,C3,C4,C5) .

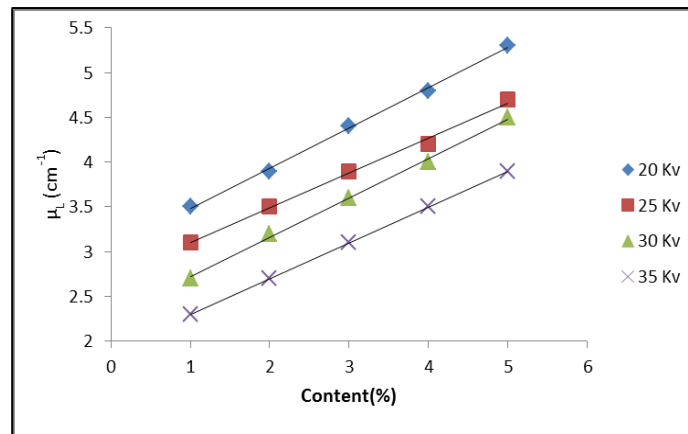


Figure 13: The relationship between the linear attenuation coefficient (μ_L) and the percentages of silver in the particle micro size of (C1,C2,C3,C4,C5) alloys at a thickness of (0.6 Cm) for the voltage range (20,25,30, 35)kv.

Figure (13) show the relationship between the linear attenuation coefficients and the silver content (micro particle) of the alloys (C1,C2,C3,C4,C5) at a pressure of (600 Mpa) at a thickness of (0.6 Cm), which increases by (33.9%) when the content is increased. Silver for alloy (B1) to alloy (B5), when comparing the results of silver content (5%) (Micro and Nano particle), it was found that the linear attenuation coefficient of alloy (B5) increases compared to the linear attenuation of alloy (C5) due to the silver content (Nano particle) compared with the sizes of the particles of the elements constituting the alloy, as the voids are filled and the inter-atomic spaces are reduced, which leads to an increase in the practical density and hardness and a decrease in porosity.

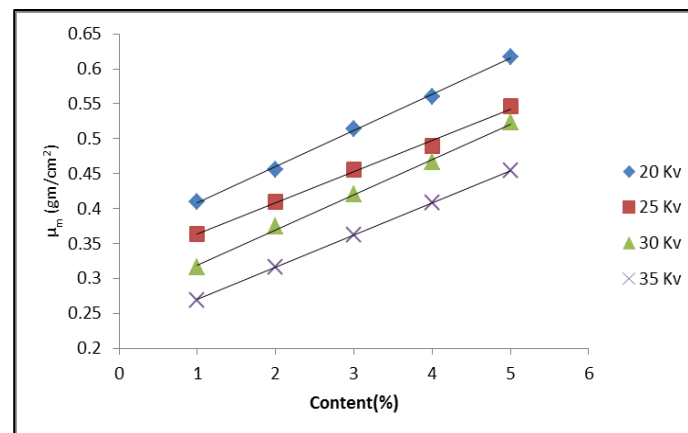


Figure 14: The relationship between the mass attenuation coefficient (μ_m) and the percentages of silver of (C1,C2,C3,C4,C5) alloys at a thickness of (0.6 Cm) for the voltage range (20,25,30, 35) Kv.

Figure (14) show the direct relationship between the mass attenuation coefficient and the silver content of the alloys (C1, C2, C3, C4, C5), as the mass attenuation coefficient increases by (33.5%) when the silver content is increased from (1-5)% to the effect of silver particles Its role is to fill in the blanks.

Conclusions

After conducting tests on the shape memory alloys (Cu - Al - Ti) we conclude the following: -

- 1- When the pressing pressure is increased (200-600) Mpa, the porosity decreases by (18%) and the hardness increases for (45%) for the base alloys from (A1) to (A5)
- 2- When the content of Nano and micro-silver is increased, the porosity of the alloys (B1) to (B5) (C1) to (C5) decreases by (39.16%) (34.69%) respectively, and the hardness increases by (32.16%) (31.3%) at the same rate relay
- 3- The linear and mass attenuation coefficients increase by (53.6%) (53.8%) for alloys from (A1) to (A5) when pressing pressure increases from (200-600) Mpa and operating voltage (20Kv).
- 4- The linear attenuation coefficient of alloys increases from (B1) to (B5) and alloys from (C1) to (C5) when the silver content of the micro particles or nanoparticles is increased and is higher compared to the mass attenuation coefficient.
- 5- The linear attenuation coefficients of (B5) and (C5) alloys are inversely proportional to the increase in the operating voltage (20-35) Kv for X-rays, as they decreased by (20%) (26.8%), respectively.
- 6- At a working voltage of (20Kv), alloy (B5) is distinguished from alloy (C5) that it has the highest linear attenuation coefficient with a decrease in porosity and an increase in hardness at compressive pressure (600Mpa) and thickness (0.6 cm).

REFERENCES

1. Jackson, D.F., Hawkes, D.J., X-ray attenuation coefficients of elements and mixtures Phys. Rep. 1981, 70, 169-233 .
2. Kaewkhao J., Laopaiboon J., Chewpraditkul W., Determination of effective atomic numbers and effective electron densities for Cu/Zn alloy, Journal of Quantitative Spectroscopy & Radioactive Transfer, 2008 Vol.109, 1260-1265.
3. A.E. Profio., " Radiation Shielding and Dosimeter " John Wiley and Sons, Inc., 1979.
4. Talb Nahe ,Alkfagy " The atom " Aldar Al Arabic Almosomat ,1989.
5. G.F.Knoll " Radiation Detection and measurement " 3rd edition ,(2000).
6. Apaydm Cengiz . G et al. "studies on mass attenuation coefficients , effective atomic number and electron densities for CoCuAg alloy " Physica Scripta, scr.79 , pp 6, 2009
7. Mohammed, Fareed .M, Razooqi, Raed . N, Ismael, Safana .M" The effect of Grain size for Aluminum and Some of its Alloys on coefficients of x-ray" in Australian journal of applied Science , Vol. 7, issue 2, Page 796-803, 2012 .
8. Mohammed, Fareed .M, Razooqi, Raed . N, Yusuf, Sokayna . E" affection of oxidation of some Aluminum Alloys on coefficients of x-ray" city Science journal , Vol. 1, issue 4, Page 33-47, 2012 .
9. Mohammed, Fareed .M, Razooqi, Raed .N, Ali, Mohsen .H" Modelling the Relation between thickness and Hardness with energy Attenuation of x-ray for pure Aluminum" in Australian journal of applied Science , Vol. 5,issue 10,Page 1268-1272, 2014 .
10. Awasarmo,Vishal.V et al. " Half and tenth value layer of some shape memory alloys the energy range 122kv to 1330kv" " International Journal of Technical , Volume 2, Issue v , page 2454-2054, 2017.
11. Dapke Gopinath .p et al. " studies on attenuation cross section parameters of some shape memory alloys in the energy range 356kev 1330kev , indian Journal of scientific research , 2018, Volume 8, Issue 1 , page 23-30.
12. Mohammed, Fareed .M, Razooqi, Raed .N, Mohammed, Mahmmod .A" Determination of the effect of oxidation on Attenuation coefficient of x-ray by Cu,Zn and their alloys " Tikrit journal of pure Science , 2018 ,Vol. 23,issue 4 , Page 107-117.
13. Mohammed, Fareed .M, Razooqi, Raed .N, Marwa, Hassan .H" studying the effect of shape memory alloys as protective shields from radiation effects in terms of attenuation coefficients of x-ray" Advances in mechanics, 2021, Vol. 9,issue 3, Page 275-290 .
14. Satish S., Malik U.S., Raju T. N.," corrosion Behavior of Cu -Zn Ni Shape Memory Alloys" Journal of minerals and material characteristics and Engineering, 2013,1, Page 49-54.
15. Kumar PK., Lagoudas D.C. (ed), " Introduction to shape memory Alloys Springer Science + business media LLCDoI: 2008 , 10.1007 / 978-0-387-47685-8-1 .
16. H. Masuda, K. Higashitani, H. Yoshida, "Powder Technology Handbook " CRC Press Taylor & Francis Group, Third Edition, 2006.
17. Razooqi, Raed Najeeb, Ahmed, saad Jeper " effect of Ag nanoparticles addition on the physical and mechanical properties of (NiTi) shape memory alloys prepared by powder metallurgy" Advances in mechanics , 2021 , Volume 9, Issue 2 , page 163-174 .
18. Razooqi, Raed Najeeb, salh, Ahmed Ismail " the effect of mixing time and method on some properties of (Al) alloy rein forced with carbon Nanotubes " International Journal of Mechanical Engineering , 2022 , Volume 7, Issue 2 , page 974-182 .
19. Razooqi, Raed Najeeb, Abdul Karim, omar Jamal " the effect of adding (mg) on the mechanical properties of the shape memory alloy (cu+Al+Ni) prepared using powder technology" tikrit journal of engineering sciences , 2020 , Volume 27, Issue 3 , page 82-93 .
20. H. Sh. Hammood, S. S. Irahayiml, A. Y. Awad and H. A. Abdulhadi" Influence of Multiwall Carbon Nanotube on Mechanical and Wear Properties of Copper – Iron Composite" International journal of Automotive and Mechanical Engineering, 2020 , Vol. 17, Page 7570 – 7576 .
21. A.B. Chilton, J.K. Shultis, and R.E. Faw., "Principles Radiation Shielding" ,Prentice - Hill, Inc ,1984.